



ELSEVIER

Journal of Non-Crystalline Solids 274 (2000) 249–256

JOURNAL OF
NON-CRYSTALLINE SOLIDS

www.elsevier.com/locate/jnoncrysol

A kinetic study on non-isothermal crystallization of the glassy alloy $\text{Sb}_{0.16}\text{As}_{0.43}\text{Se}_{0.41}$

P.L. López-Alemany, J. Vázquez *, P. Villares, R. Jiménez-Garay

Departamento de Física de la Materia Condensada, Facultad de Ciencias, Universidad de Cádiz, Apartado 40, 11510 Puerto Real (Cádiz), Spain

Abstract

A procedure has been used for analyzing the evolution with time of the volume fraction crystallized and for calculating the kinetic parameters at non-isothermal reactions in materials involving formation and growth of nuclei. Considering the assumptions of extended volume and random nucleation, a general expression of the fraction crystallized has been obtained as a function of the temperature for interior crystallization. The kinetic parameters have been deduced, assuming that the crystal growth rate has an Arrhenius-type temperature dependence, and the nucleation frequency is either constant or negligible. The theoretical method described has been applied to the crystallization kinetics of glassy alloy $\text{Sb}_{0.16}\text{As}_{0.43}\text{Se}_{0.41}$ with and without previous reheating. According to the study carried out, the values of the kinetic exponent, n , are 1.8 for the as-quenched glass and 0.9 for the reheated glass. As n decreases with reheating, it is possible to state that the annealing causes the appearance of new nuclei. The phases at which the alloy crystallizes after the thermal process have been identified by X-ray diffraction. Based on the diffractogram of the transformed material we suggest the presence of microcrystallites of Sb_2Se_3 and AsSe , remaining in the amorphous matrix. © 2000 Elsevier Science B.V. All rights reserved.

1. Introduction

An understanding of the kinetics of crystallization in glasses is important for the manufacturing of glass-ceramics and in preventing devitrification. Nucleation and crystallization rates are sometimes measured directly in the microscope [1] but this method could not be applied to glasses in which nucleation and crystallization occurred in times below 1 h. Differential scanning calorimetry (DSC) is valuable for the quantitative study of crystallization in different glassy systems. This

study of crystallization kinetics has been widely discussed in the literature [2–5]. Many authors used the so-called Kissinger plot [5] or Ozawa plot [6] directly to examine the kinetics of crystallization of amorphous materials. These methods, however, cannot be directly applied to the crystallization of amorphous materials and the physical meaning of the activation energies thus obtained are obscure because the crystallization is advanced not by the n th-order reaction but by the nucleation and growth processes. On the other hand, some authors applied the Johnson–Mehl–Avrami (JMA) [7–9] equation to the non-isothermal crystallization process [10–12]. Although sometimes they appeared to get reasonable activation energies, this procedure is not appropriate when their expressions are deduced from the JMA

* Corresponding author. Tel.: +34-956 830 966; fax: +34-956 834 924.

E-mail address: wagner@merlin.eca.es (J. Vázquez).

equation considering isothermal crystallization conditions [13].

In this work, an analysis of the non-isothermal crystallization kinetics is described on the basis of nucleation and crystal growth processes, and it is emphasized that the crystallization mechanism, such as interior crystallization, should be taken into account for obtaining a meaningful activation energy. In addition, the present paper applies the quoted analysis to the thermal treatment of the glassy alloy $\text{Sb}_{0.16}\text{As}_{0.43}\text{Se}_{0.41}$. Thus, it is possible to state that reheating produces new nuclei. Finally, the crystalline phases corresponding to the crystallization process were identified by X-ray diffraction (XRD) measurements, using CuK_α radiation.

2. Theoretical background

2.1. Nucleation, crystal growth and volume fraction crystallized

The theoretical basis for interpreting DSC results is provided by the formal theory of transformation kinetics [7–9,14–17]. Defining an extended volume of transformed material and assuming spatially random nucleation [18,19] the crystallized volume fraction is expressed as

$$x = 1 - \exp(-x_{\text{ext}}). \quad (1)$$

Here x_{ext} represents the ‘extended’ volume fraction (i.e., the one which the crystallites would occupy in the absence of interaction or overlap). The evolution with time, t , of the fraction, x_{ext} , in terms of the nucleation frequency (per unit volume), I_V , and the crystal growth rate u , is described as

$$x_{\text{ext}}(t) = g \int_0^t I_V(\tau) \left[\int_\tau^t u(t') dt' \right]^m d\tau, \quad (2)$$

where g is a geometric factor, τ is the time in which an individual region is nucleated, and m is an exponent which depends on the dimensionality of the crystal growth.

In non-isothermal experiments of interior crystallization with a quenched glass containing no nuclei, assuming that the crystal growth rate

has an Arrhenian temperature dependence, $u = u_0 \exp(-E/RT)$, Eq. (1) becomes

$$\begin{aligned} & -\ln(1-x) \\ &= \frac{gu_0^3}{\beta^3} \int_0^t I_V(\tau) \left[\int_{T_\tau}^T \exp(-E/RT') dT' \right]^3 d\tau \\ &= \frac{C_1}{\beta^3} \int_0^t I_V(\tau) I_1^3 d\tau, \end{aligned} \quad (3)$$

where T_τ is the corresponding temperature at time τ , $\beta = dT'/dt'$ the heating rate and E being the activation energy. Using the substitution $y' = E/RT'$, the integral I_1 is transformed to the relationship

$$I_1 = (E/R) \int_y^{y_\tau} e^{-y'} y'^{-2} dy' \quad (4)$$

which is not integrable in closed form and is represented in the literature [20] by several approximate analytical expressions. The authors Vázquez et al. [21] have expressed Eq. (4) by an alternating series, resulting in

$$I_1 = \frac{E}{R} \left[-e^{-y'} y'^{-2} \sum_{k=0}^{\infty} \frac{(-1)^k (k+1)!}{y'^k} \right]_y^{y_\tau}, \quad (5)$$

where it is possible to use only the first term, without making any appreciable error and thus justifying the approximation

$$I_1 = (E/R) e^{-y} y^{-2} \quad (6)$$

if it is assumed that $T_\tau \ll T$, so that y_τ can be taken as infinity and, of course $y \gg 1$ (i.e. $E \gg RT$) [20]. Given that, asymptotically, for $E \gg RT$ the exponential term in Eq. (6) changes much faster compared to the power law, the latter can be treated almost as a constant and then the Eq. (6) can be written as

$$I_1 \approx A_1 e^{-y} = A_1 \exp(-E/RT). \quad (7)$$

Substituting Eq. (7) in Eq. (3) with the assumption that the nucleation frequency is practically constant and integrating the resulting expression, we obtain

$$\begin{aligned}
 -\ln(1-x) &= \frac{C_2}{\beta^4} I_V(T - T_0) \exp(-3E/RT) \\
 &= \frac{C_2 N_0}{\beta^4} \exp(-3E/RT), \tag{8}
 \end{aligned}$$

where N_0 being the nuclei formed per unit volume in the course of the thermal process at the heating rate, β , that is, the area under the nucleation curve.

In the case of a glass which has been heated previously at the temperature of maximum nucleation rate for sufficiently long time, a large number of nuclei already exist and no new nuclei are formed during the thermal process (i.e. $I_V = 0$). Therefore, from Eqs. (1) and (2), the following expression can be obtained:

$$-\ln(1-x) = gN \left[\int_0^t u(t') dt' \right]^3 = \frac{C_1 N}{\beta^3} I_2^3, \tag{9}$$

N being the number of nuclei per unit volume, and where the integral has been evaluated between 0 and t , since there is no nucleation period, $\tau = 0$. The integral I_2 has been resolved in the same manner as I_1 , and substituting the resulting expression in Eq. (9), yields

$$-\ln(1-x) = \frac{C_2 N}{\beta^3} \exp(-3E/RT). \tag{10}$$

Eqs. (8) and (10) may be expressed by the more general relationship

$$-\ln(1-x) = C_0 \beta^{-n} \exp(-mE/RT). \tag{11}$$

Here, $n = m + 1$ for a quenched glass containing no nuclei and $n = m$ for a glass containing a number of nuclei close to the one corresponding to the ‘site saturation’ condition.

2.2. Calculating kinetic parameters

The usual analytical methods, proposed in the literature for analyzing the transformation kinetics, assume that the reaction rate constant can be defined by an Arrhenian temperature dependence. In order for this condition to hold, the present work assumes that the crystal growth rate, u , has an Arrhenian temperature dependence, and over the temperature range where the thermoanalytical

measurements are carried out, the nucleation rate is either constant or negligible (i.e., the condition of site saturation). From this point of view, the crystallization rate is obtained by deriving the volume fraction crystallized with respect to time, yielding

$$\left. \frac{dx}{dt} \right|_p = K_1 \beta^{-(n-1)} (1-x_p) \exp(-mE/RT_p). \tag{12}$$

The maximum crystallization rate is found by making $dx^2/dt^2 = 0$, thus obtaining the relationship

$$\left. \frac{dx}{dt} \right|_p = mE\beta(1-x_p)/RT_p^2. \tag{13}$$

Eqs. (12) and (13) have been deduced taking a sufficiently limited range of temperature (such as the range of crystallization peaks in DSC experiments) so that the fraction, $1/T^2$, can be considered practically constant, and designating with the subscript, p , the magnitudes corresponding to the maximum crystallization rate. Relating the above-mentioned equations and taking the logarithm leads to the relationship

$$\ln \left(\frac{T_p^2}{\beta^n} \right) = \frac{mE}{R} \frac{1}{T_p} + \text{constant}, \tag{14}$$

which is a linear function, whose slope yields the product, mE , of the process.

The use of Eq. (14) implies a previous knowledge of the kinetic exponent, n , which can be obtained taking the logarithm of Eq. (11), yielding

$$\begin{aligned}
 z &= \ln[-\ln(1-x)] \\
 &= -n \ln \beta - mE/RT + \ln C_0 \tag{15}
 \end{aligned}$$

and representing z versus $\ln \beta$ at a specific temperature. One method for determining the m is to observe the change of n with reheating at the nucleation temperature (slightly higher than the glass transition temperature, T_g). If n does not change with reheating, then the initial number of nuclei in the specimen must be close to the one corresponding to site saturation condition, and $n = m$. If n decreases with reheating, then the initial number of nuclei might be much lower. In this case, $m < n \leq m + 1$ before reheating and $n = m$ after reheating.

3. Experimental

The semiconducting $\text{Sb}_{0.16}\text{As}_{0.43}\text{Se}_{0.41}$ glassy was made from their components of 99.999 purity, which were pulverized to less than $64\ \mu\text{m}$, mixed in adequate proportions, and introduced into quartz ampoules. The ampoules were subjected to an alternating process of filling and evacuation of inert gas, to ensure the absence of oxygen. This process ended with a final evacuation of up to $10^{-2}\ \text{N m}^{-2}$, and sealing with an oxyacetylene burner. The ampoules were put into a furnace at around $1225\ \text{K}$ for 24 h, turning at $1/3\ \text{rpm}$, to improve homogeneity of the molten material, and then the ampoule was quenched in water to avoid crystallization. The capsules containing the samples were then put into a mixture of hydrofluoric acid and hydrogen peroxide to corrode the quartz and make it easier to extract the alloy. The amorphous state of the material was confirmed by a diffractometric X-ray scan (Siemens D500), showing an absence of the peaks which are characteristic of crystalline phases. The homogeneity and composition of the samples were verified through scanning electron microscopy (JSM-820). The calorimetric measurements were carried out in a differential scanning calorimeter (Perkin–Elmer DSC7) with an accuracy of $\pm 0.1\ \text{K}$, keeping a constant flow of nitrogen to extract the gases generated during the crystallization reactions, which, as is characteristic of chalcogenide materials, corrode the DSC sensor equipment. The calorimeter was calibrated, for each heating rate, using the well-known melting temperatures and melting enthalpies of zinc and indium supplied with the instrument [22]. The analyzed samples, were pulverized (particle size around $40\ \mu\text{m}$), crimped into aluminium pans, and their masses were about $20\ \text{mg}$. An empty aluminium pan was used as reference. The crystallization experiments were carried out through continuous heating at rates, β of 2, 4, 8, 16, 32 and $64\ \text{K min}^{-1}$. The glass transition temperature was considered as a temperature corresponding to the inflection point of the lambda-like trace on the DSC scan, as shown in Fig. 1. The crystallized fraction, x , at any temperature T is given as $x = A_T/A$, where A is the total area of the exo-

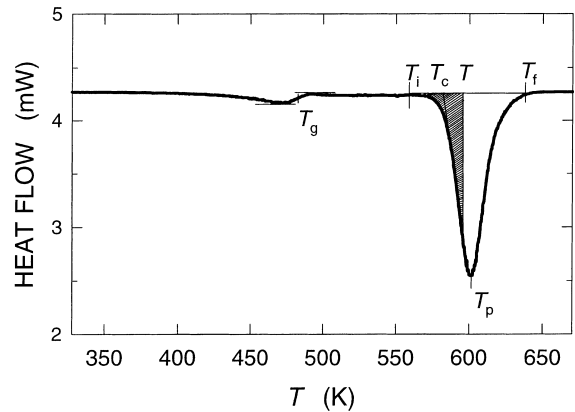


Fig. 1. Typical DSC trace of $\text{Sb}_{0.16}\text{As}_{0.43}\text{Se}_{0.41}$ glassy alloy at a heating rate of $16\ \text{K min}^{-1}$. The hatched area shows A_T , the area between T_i and T .

therm between the temperature T_i , where the crystallization is just beginning and the temperature T_f , where the crystallization is completed and A_T is the area between the initial temperature and a generic temperature T , see Fig. 1. With the aim of investigating the phases into which the samples crystallize, diffractograms of the material transformed after the thermal treatment were obtained. The experiments were performed with a diffractometer Philips (type PW 1830). The patterns were run with Cu as target and Ni as filter ($\lambda = 1.542\ \text{\AA}$) at $40\ \text{kV}$ and $40\ \text{mA}$, with a scanning speed of $0.1^\circ\ \text{s}^{-1}$.

4. Results

The DSC curve for sample obtained at a heating rate of $16\ \text{K min}^{-1}$ and plotted in Fig. 1 make it possible to determine the glass transition temperature, $T_g = 483.2 \pm 2.1\ \text{K}$, the extrapolated onset crystallization temperature, $T_c = 580.4 \pm 2.5\ \text{K}$, and the peak temperature of crystallization, $T_p = 600.2 \pm 2.6\ \text{K}$. This DSC trace shows the typical glass–crystal transformation. The DSC data for the different heating rates, β , quoted in Section 3, show T_g s, T_c s, and T_p s which increase with increasing β , a property which has been reported in the literature [23].

4.1. The crystallization

The kinetic analysis of the crystallization reactions is related to the knowledge of the reaction rate constant, K , as a function of the temperature. In the present work it is assumed that the constant, K , has an Arrhenius type temperature dependence. Bearing in mind this assumption and that the nucleation frequency is practically constant, as supposed in this work, the overall effective activation energy is related to the activation energy for crystal growth by the ratio m/n . From this point of view, and considering that in most crystallization processes $E \gg RT$, the crystallization kinetics of the alloy $\text{Sb}_{0.16}\text{As}_{0.43}\text{Se}_{0.41}$ may be analyzed according to the appropriate approximation described in Section 2.

With the aim of analyzing the above-mentioned kinetics, the variation intervals of the magnitudes described by the thermograms for the different heating rates quoted in Section 3 are obtained and given in Table 1, where T_i and T_p are the temperatures at which crystallization begins and that corresponding to the maximum crystallization rate, respectively, and ΔT is the width of the crystallization peak. The crystallization enthalpy, ΔH , is also determined for each of the heating rates. The crystallization rates corresponding to the different scans are represented in Fig. 2. We observe that $(dx/dt)_p$ increase in the same proportion as the heating rate, a property which has been discussed in the literature [23].

For the purpose of correctly applying the preceding theory, the material was reheated up to 516 K (a temperature slightly higher than T_g) for 1 h to form a larger number of nuclei. We ascertained by

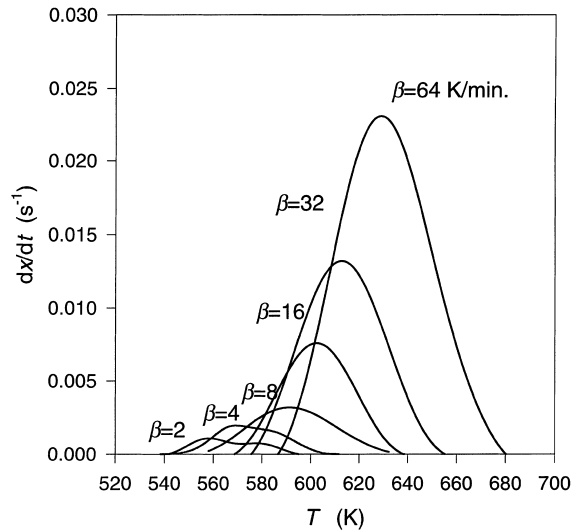


Fig. 2. Crystallization rate versus temperature of the exothermal peak at different heating rates.

X-ray diffraction that no crystalline peaks were detected after the annealing. From the experimental data the plots of $z = \ln[-\ln(1-x)]$ versus $\ln \beta$ at different specific temperatures has been drawn, both for the as-quenched glass and for the reheated glass. We observed that the correlation coefficients of the corresponding straight regression lines were a maximum for a given temperature, which was considered as the most adequate one for the calculation of parameter n . Fig. 3 shows the relation between z and $\ln \beta$ for as-quenched glass at 590.1 K and reheated glass at 580.2 K. According to Eq. (15), the slopes of these functions give the ns , and we found that $n = 1.8 \pm 0.3$ for the as-quenched glass and $n = 0.9 \pm 0.1$ for the reheated glass. Allowing for experimental error, these ns are close to 2 and 1, respectively. These ns indicate that the reheating has produced new nuclei, and therefore $m = 1$, that is, the crystal particles grow one dimensionally.

Once the crystallization mechanism is known, according to Eq. (14) it is possible to draw the plots in Fig. 4, which show the variation of $\ln(T_p^2/\beta^n)$ versus $1/T_p$. The slopes of the obtained functions by least squares fitting to data of $\ln(T_p^2/\beta^n)$ and $1/T_p$ give the activation energy for crystallization process: $34.0 \pm 1.2 \text{ kcal mol}^{-1}$ for

Table 1

Variation intervals of the characteristic temperatures and enthalpies of the crystallization process of alloy $\text{Sb}_{0.16}\text{As}_{0.43}\text{Se}_{0.41}$ for different heating rates

Parameters	Experimental	
	As-quenched	Reheated
T_g (K)	469–493	468–495
T_i (K)	540–584	519–549
T_p (K)	566–625	554–608
ΔT (K)	52–99	71–131
ΔH (mcal mg^{-1})	8–11	8–10

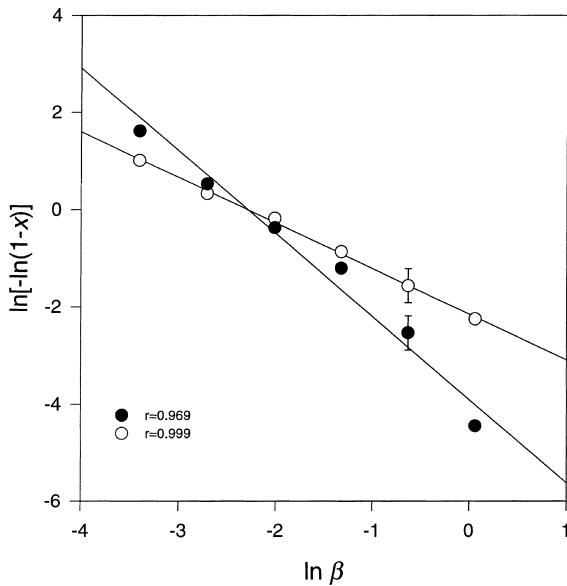


Fig. 3. Variation of $\ln[-\ln(1-x)]$ with logarithm of heating rate (β in K s^{-1}): ● as-quenched glass at 590.1 K; ○ reheated glass at 580.2 K.

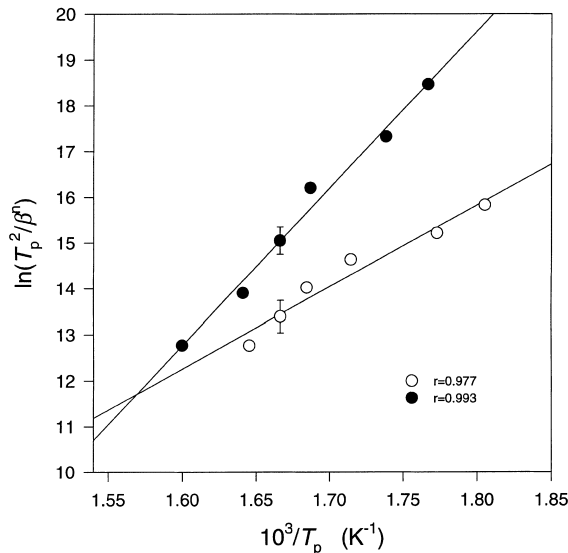


Fig. 4. Experimental plot of $\ln(T_p^2/\beta^n)$ versus $10^3/T_p$ and straight regression lines of $\text{Sb}_{0.16}\text{As}_{0.43}\text{Se}_{0.41}$ alloy (β in K s^{-1}).

the reheated glass, and $65.2 \pm 1.8 \text{ kcal mol}^{-1}$ for the as-quenched glass. On the other hand, taking the logarithm of Eq. (11) we obtain the expression

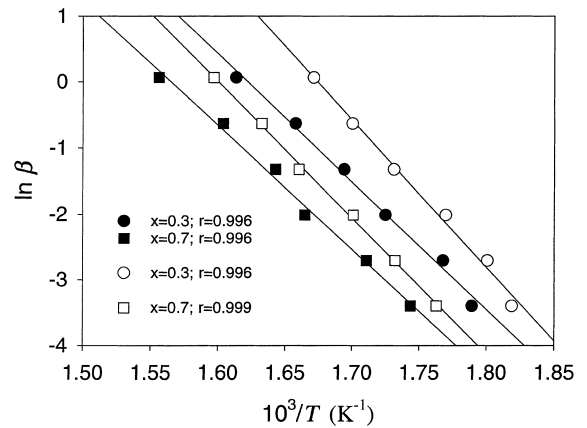


Fig. 5. Plot of $\ln \beta$ versus $10^3/T$ for the values of the volume fraction crystallized equal to 0.3 and 0.7 (β in K s^{-1}): ● as-quenched glass; ○ reheated glass.

Table 2

Activation energy obtained from the plot of $\ln \beta$ versus $1/T$ for given values of the volume fraction crystallized

Volume fraction crystallized	E (kcal mol^{-1})	
	As-quenched glass	Reheated glass
0.3	62.7 ± 1.7	39.8 ± 1.0
0.7	60.8 ± 1.7	36.8 ± 1.3
x_p	67.5 ± 2.4	36.1 ± 1.1

$$\ln \beta = -\frac{m}{n} \frac{E}{RT} - \frac{1}{n} \ln[-\ln(1-x)] + \text{constant}, \quad (16)$$

which permits representation of $\ln \beta$ versus $1/T$ for a specific volume fraction crystallized, and E being the activation energy of the transformation. Fig. 5 shows the relation between $\ln \beta$ and the reciprocal temperature at which x reaches 0.3 and 0.7. According to Eq. (16) this plot should give the E s, for as-quenched glass and for reheated glass, which are shown in Table 2. Finally, assuming that the volume fraction crystallized at T_p is practically the same irrespective of β , and using Eq. (16) we obtain the activation energies, which are also given in Table 2.

We observe that the activation energies obtained for as-quenched glass and for reheated glass differ which confirms, together with the n s, that the

annealing produces new nuclei. From the mean of the kinetic exponent $\langle n \rangle = 2$, and according to the Avrami theory of nucleation, we state that in the crystallization reaction mechanism there is diffusion-controlled growth. In addition, according to the usual criteria [24,25] for the interpretation of n , some observations relating to the morphology of the growth can be worked out. In the glassy alloy $\text{Sb}_{0.16}\text{As}_{0.43}\text{Se}_{0.41}$ as-quenched there is a relatively stable crystalline phase ($\langle E \rangle = 64 \text{ kcal mol}^{-1}$), with an interior nucleation mechanism. According to the literature [24], the phase may be due to an initial growth of particles nucleated at constant rate, since the mean of the kinetic exponent is included in the interval 1.5–2.5.

5. Identification of the crystalline phases

Taking into account the crystallization exothermal peaks observed in the DSC data of the $\text{Sb}_{0.16}\text{As}_{0.43}\text{Se}_{0.41}$ sample we try to identify the possible phases that crystallize during the thermal treatment by means of XRD measurements. For this purpose, in Fig. 6 we show the most relevant portions of the diffractometer tracings for the as-quenched sample and for the annealed sample. Fig. 6(A) has maxima observed in XRD of the amorphous phase of the starting material at diffraction angles (2θ) between 20° and 60° . Based on the diffractogram of the transformed material after the crystallization process (Fig. 6(B)) we suggest the presence of crystallites of Sb_2Se_3 and AsSe indicated with \bullet and \circ , respectively, while

there remains also a residual amorphous phase. The Sb_2Se_3 phase crystallizes in the orthorhombic system with a unit cell defined by $a = 11.633 \text{ \AA}$, $b = 11.78 \text{ \AA}$ and $c = 3.895 \text{ \AA}$ [26].

6. Conclusions

Our theoretical method enables us to study the evolution with time of the volume fraction crystallized in materials involving nucleation and crystal growth processes. This procedure assumes an extended volume of transformed material and random nucleation. Using these assumptions we have obtained a general expression of the volume fraction crystallized, as a function of temperature in interior crystallization processes. We conclude that the numerical factors, n and m depend on the mechanism of nucleation and growth, and the dimensionality of the crystal. In addition we found that, $n = m + 1$ for a quenched glass containing no nuclei while $n = m$ for a glass containing a large number of nuclei. The kinetic parameters were deduced based on a maximum crystallization rate. For the alloy $\text{Sb}_{0.16}\text{As}_{0.43}\text{Se}_{0.41}$, with and without previous reheating, we establish that the reheating causes the appearance of new nuclei. The proposed method for the thermal analysis of this alloy has given results in agreement with the properties of the material under study. The value found for the kinetic exponent of the as-quenched glass is consistent with a mechanism of volume nucleation and one-dimensional growth. Finally, we have identified the crystalline phases from the XRD

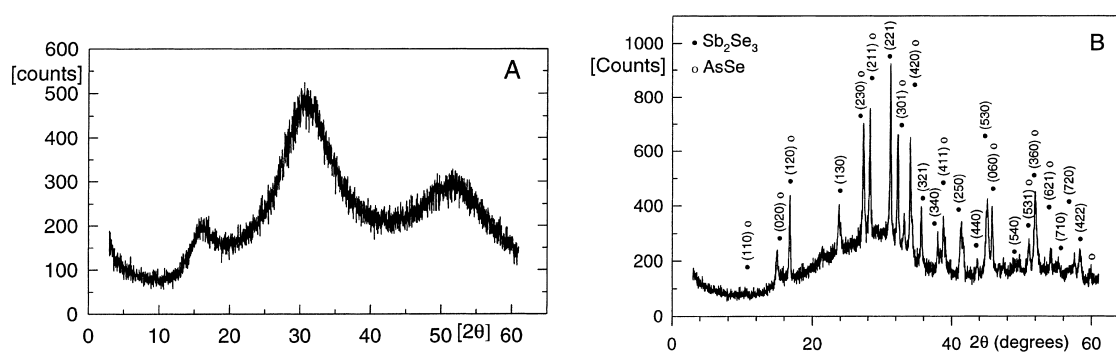


Fig. 6. (A) Diffractogram of amorphous alloy $\text{Sb}_{0.16}\text{As}_{0.43}\text{Se}_{0.41}$. (B) Diffraction peaks of alloy crystallized in DSC.

pattern of the transformed material and suggest the existence of crystallites of Sb_2Se_3 and AsSe remaining in the amorphous matrix.

Acknowledgements

The authors are grateful to the Junta de Andalucía and the CICYT (Comisión Interministerial de Ciencia y Tecnología) (Project no. MAT98-0791) for their financial support.

References

- [1] N.P. Bansal, R.H. Doremus, A.J. Bruce, C.T. Moynihan, *J. Am. Ceram. Soc.* 66 (1983) 233.
- [2] D.W. Henderson, *J. Non-Cryst. Solids* 30 (1979) 301.
- [3] K.F. Kelton, *Crystal Nucleation in Liquids and Glasses*, Solid State Physics, vol. 45, Academic Press, New York, 1991.
- [4] N. Clavaguera, *J. Non-Cryst. Solids* 162 (1993) 40.
- [5] H.E. Kissinger, *Anal. Chem.* 29 (1957) 1702.
- [6] T. Ozawa, *J. Thermal Anal.* 2 (1970) 301.
- [7] M. Avrami, *J. Chem. Phys.* 7 (1939) 1103.
- [8] M. Avrami, *J. Chem. Phys.* 8 (1940) 212.
- [9] M. Avrami, *J. Chem. Phys.* 9 (1941) 177.
- [10] J. Colmenero, J. Ilarraz, *Termochim. Acta* 35 (1980) 381.
- [11] A. Marotta, S. Saiello, F. Branda, A. Buri, *J. Mater. Sci.* 17 (1982) 105.
- [12] K. Harnisch, R. Lanzenberger, *J. Non-Cryst. Solids* 53 (1982) 235.
- [13] M.E. Fine, *Introduction to Phase Transformation in Condensed System*, Macmillan, New York, 1964 (Chapter 3).
- [14] A.N. Kolmogorov, *Bull. Acad. Sci. USSR (Sci. Mater. Nat.)* 3 (1937) 3551.
- [15] W.A. Johnson, R.F. Mehl, *Trans. AIME* 135 (1939) 416.
- [16] M.C. Weinberg, R. Kapral, *J. Chem. Phys.* 91 (1989) 7146.
- [17] V. Erukhimovitch, J. Baram, *J. Non-Cryst. Solids* 208 (1996) 288.
- [18] J. Vázquez, P. Villares, R. Jiménez-Garay, *J. Alloys Compounds* 257 (1997) 259.
- [19] V.A. Shneidman, D.R. Uhlmann, *J. Chem. Phys.* 109 (1998) 186.
- [20] H. Yinnon, D.R. Uhlmann, *J. Non-Cryst. Solids* 54 (1983) 253.
- [21] J. Vázquez, C. Wagner, P. Villares, R. Jiménez-Garay, *Acta Mater.* 44 (1996) 4807.
- [22] Perkin Elmer, PC Series, Thermal Analysis System, DSC 7 Differential Scanning Calorimeter, Operator's Manual, Norwalk, Connecticut, 1989.
- [23] J. Vázquez, P.L. López-Alemaný, P. Villares, R. Jiménez-Garay, *Mater. Chem. Phys.* 57 (1998) 162.
- [24] C.N.R. Rao, K.J. Rao, *Phase Transition in Solids*, McGraw-Hill, New York, 1978.
- [25] R. Chiba, N. Funakoshi, *J. Non-Cryst. Solids* 105 (1988) 149.
- [26] S.A. Dembovski, *Russ. J. Inorg. Chem.* 8 (1963) 798 (English Trans.).